Reelin is a target of polyglutamine expanded ataxin-7 in human spinocerebellar ataxia type 7 (SCA7) astrocytes

Shaun D. McCullough[a], Xiaojiang Xu[a], Sharon Y. R. Dent[b], Stefan Bekiranov[a], Robert G. Roeder[c,1], and Patrick A. Grant[a,1]

[a]Department of Biochemistry and Molecular Genetics, University of Virginia School of Medicine, Charlottesville, VA 22908; [b]Department of Molecular Carcinogenesis at the Virginia Harris Cockrell Cancer Research Center, University of Texas M. D. Anderson Cancer Center, Smithville, TX 78957; and [c]Laboratory of Biochemistry and Molecular Biology, The Rockefeller University, New York, NY 10065

Contributed by Robert G. Roeder, November 13, 2012 (sent for review June 6, 2012)

Spinocerebellar ataxia type 7 (SCA7) is an autosomal-dominant neurodegenerative disorder that results from polyglutamine expansion of the ataxin-7 (ATXN7) protein. Remarkably, although mutant ATXN7 is expressed throughout the body, pathology is restricted primarily to the cerebellum and retina. One major goal has been to identify factors that contribute to the tissue specificity of SCA7. Here we describe the development and use of a human astrocyte cell culture model to identify reelin, a factor intimately involved in the development and maintenance of Purkinje cells and the cerebellum as a whole, as an ATXN7 target gene. We found that polyglutamine expansion decreased ATXN7 occupancy, which correlated with increased levels of histone H2B monoubiquitination, at the reelin promoter. Treatment with trichostatin A, but not other histone deacetylase inhibitors, partially restored reelin transcription and promoted the accumulation of mutant ATXN7 into nuclear inclusions. Our findings suggest that reelin could be a previously unknown factor involved in the tissue specificity of SCA7 and that trichostatin A may ameliorate deleterious effects of the mutant ATXN7 protein by promoting its sequestration away from promoters into nuclear inclusions.

chromatin | SAGA complex | histone modification

As a member of the polyglutamine expansion disorder family, Spinocerebellar ataxia type 7 (SCA7) is an autosomal-dominant hereditary disease characterized by cerebellar and retinal degeneration eventually leading to death (1). Although the ataxin-7 (ATXN7) protein is expressed throughout the body, pathology is localized primarily within the cerebellum and retina. Cerebellar Purkinje cell (PC) degeneration is an integral step in the development and progression of SCA7 and has been observed in several independent transgenic mouse models of the disease (2–5); however, increasing evidence indicates that glial cell dysfunction contributes significantly to polyglutamine expansion disorder pathology (2, 6, 7). Interestingly, two distinct SCA7 mouse models exhibit non–cell-autonomous neurodegeneration (2, 4). Of these, the model used by Custer et al. (2) demonstrates that astrocyte-specific expression of polyQ ATXN7, via the *Gfa2* promoter (8), results in PC degeneration and the onset of SCA7 symptoms. Astrocytes play a crucial role in the regulation of synaptic formation and function by ensheathing axon–dendrite connections to form a structure known as the tripartite synapse (9). This intimate interaction allows astrocytes to modulate synaptic function through the release of chemical messengers and the regulation of neurotransmitter and ion concentration within the synapse (9–11). The identification of tissue specificity factors and characterization of associated molecular mechanisms involved in their deregulation will facilitate a more comprehensive understanding of disease-associated events and advance efforts to develop effective treatments.

The ATXN7 protein is an integral subunit of GCN5 (general control of amino acid synthesis-5; KAT2A)-containing SAGA family of histone acetyltransferase (HAT) complexes (hereafter referred to collectively as the SAGA complex) from budding yeast to humans (12, 13). Incorporation of the polyQ ATXN7 protein into SAGA results in the loss of several subunits and disruption of its nucleosomal acetyltransferase activity (12, 13). Several studies have examined the effect of polyQ ATXN7 expression on the regulation of individual target genes; however, the impact of mutant ATXN7 expression on global gene expression in astrocytes has not yet been examined. As a result, we sought to develop a tissue culture system with which we could characterize polyQ ATXN7-dependent alterations to gene expression and chromatin modification in human astrocytes that may contribute to non–cell-autonomous neurodegeneration in SCA7. Here we characterize the association between expression of mutant ATXN7 and regulation of the reelin (RELN) gene, which plays a critical role in cerebellar development and PC maintenance (14–16), in a SCA7 astrocyte model.

Results

Construction of SCA7 Astrocyte Cell Culture Model. To study the effects of mutant ATXN7 protein expression on human astrocytes, we generated recombinant lentiviral particles in HEK293T/17 cells with the pSDM253 and pSDM254 lentiviral transfer vectors to deliver the WT (24Q) and polyQ (92Q) ATXN7 transgenes to artificially immortalized astrocytes (17). The transfer vectors also contained an EGFP gene, which served as a marker for the identification of transduced cells. Transduced astrocyte populations exhibited consistently high rates of EGFP-positive cells—95.4% and 96.0% for F-ATXN7/24Q and F-ATXN7/92Q cells, respectively—as measured by flow cytometry (Fig. 1*A*). Further, the percentage of cells expressing the exogenous Flag-ATXN7 protein, as determined by immunostaining with anti-Flag antibodies, was similar to the percentage of EGFP-positive cells in the population (Fig. 1*A*). These results indicated that our transduction conditions allowed for the production of populations in which nearly all cells expressed exogenous ATXN7 protein.

After establishing efficient transduction conditions, we confirmed that the exogenous ATXN7 proteins were expressed at their expected molecular weights by Western blot analysis (Fig. 1*B*). A high molecular weight band was apparent in polyQ ATXN7-expressing cells by 6 d postinfection, which we believe represents ATXN7 aggregates known as nuclear inclusions (NIs; Fig. 1*B*). The formation of NIs is a hallmark of polyglutamine expansion

Author contributions: S.Y.R.D. and P.A.G. designed research; S.D.M. performed research; S.D.M., S.B., and R.G.R. contributed new reagents/analytic tools; S.D.M., X.X., S.B., R.G.R., and P.A.G. analyzed data; and S.D.M. and P.A.G. wrote the paper.

The authors declare no conflict of interest.

[1]To whom correspondence may be addressed. E-mail: roeder@rockefeller.edu or pag9n@virginia.edu.

This article contains supporting information online at www.pnas.org/lookup/suppl/doi:10.1073/pnas.1218331110/-/DCSupplemental.

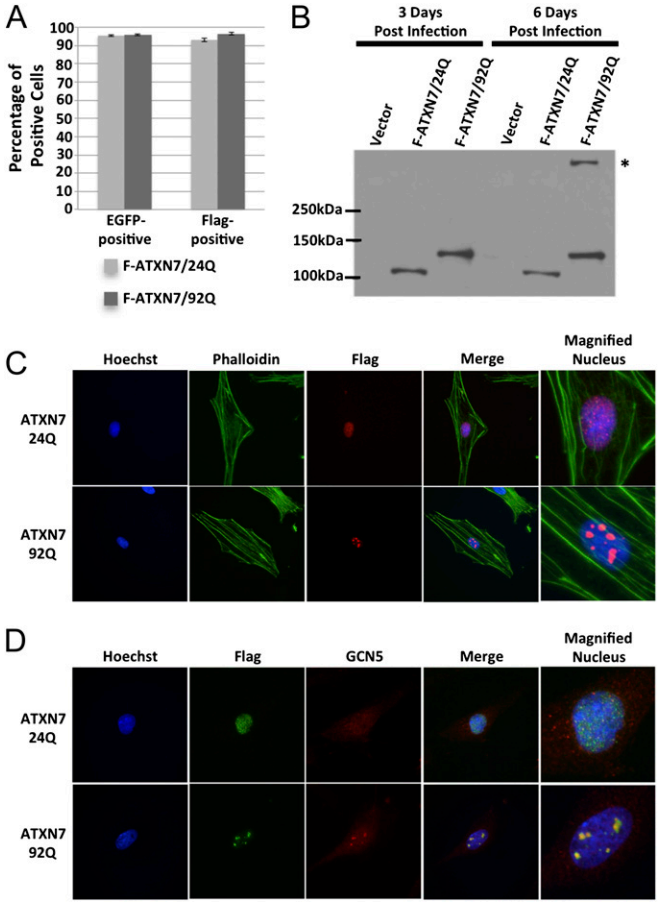

Fig. 1. Establishment of a recombinant lentiviral delivery system for the stable expression of ATXN7 in cultured human astrocytes. (*A*) The percentage of transduced cells (EGFP-positive) was similar to the percentage of cells expressing exogenous F-ATXN7 (Flag-positive). (*B*) Expression of exogenous ATXN7 proteins in WCE from SCA7 astrocytes was confirmed by immunoblot with anti-Flag antibodies at 3 and 6 d postinfection. Exogenous Flag-ATXN7 proteins were observed at expected molecular weights. SDS-insoluble aggregates (asterisk) were present at time points by 6 d postinfection in mutant SCA7 astrocytes. (*C*) Formation of NIs in cells expressing the polyQ ATXN7 protein was confirmed by immunofluorescence staining of infected astrocytes with anti-Flag antibodies. Cell bodies and nuclei were visualized with phalloidin (green) and Hoechst dye (blue), respectively. (*D*) GCN5 colocalization with NIs in mutant SCA7 astrocytes was observed by immunofluorescence staining of SCA7 astrocytes with anti-Flag and anti-GCN5 antibodies. Cell nuclei were visualized by Hoechst dye (blue).

disorders (18); however, the role of these inclusions in disease progression remains unclear. To confirm that the polyQ ATXN7 aggregates, observed as high molecular weight bands in Fig. 1*B*, were bona fide NIs, transduced astrocytes were examined by immunofluorescence microscopy after staining with anti-Flag antibodies (Fig. 1*C*). Quantification of immunostaining results indicated that NIs formed in 20.6% of cells expressing the mutant ATXN7 protein ($n = 725$ cells counted, SEM ± 1.7%), but were absent in those expressing its WT counterpart ($n = 676$ cells counted). To further highlight the similarities between our SCA7 astrocyte model and previously reported SCA7 patient and laboratory model data (4, 5, 19), we observed an apparent polyQ-dependent increase in ATXN7 protein stability (Fig. 1*B*).

Given their heterogeneous nature (3, 19) and the association of ATXN7 with SAGA, we assessed whether GCN5 was present within NIs in our SCA7 astrocyte model. Simultaneous immunostaining with anti-Flag and anti-GCN5 antibodies demonstrated the colocalization of GCN5 into at least one NI in 53.8% of astrocytes containing ATXN7 aggregates (SEM ± 4.77%, $n = 725$; Fig. 1*D*). Aggregates containing GCN5 were often larger compared with those lacking GCN5, suggesting that the incorporation of other proteins into these inclusions may not be part of their nucleation, occurring instead at later phases of their formation. All these data indicate that the SCA7 astrocyte model we have developed exhibits the basic characteristics of cells that would be present in SCA7 individuals, thus serving as an appropriate tissue culture model for studying effects of the polyQ ATXN7 protein on astrocyte function.

Transcriptional Alterations in Astrocytes Expressing polyQ ATXN7 Protein. The SAGA complex family regulates the transcription of target genes through several catalytic functions (20–23). Given previous observations demonstrating the disruption of SAGA complex activity (12, 13), we sought to identify transcriptional alterations that resulted from expression of the polyQ ATXN7 protein. Analysis of our microarray results indicated that 21 coding genes (Table S1) and eight noncoding RNAs (Table S2) were differentially expressed in Flag-ATXN7/92Q (mutant SCA7) astrocytes. Of the 21 coding genes identified, nearly half have been previously associated with neurologic development, maintenance, or disease (*CYR61*, *LGR4*, *GPR56*, *SLC1A4*, *SERPINE2*, *EPHA5*, *RELN*, *PTGS1*, and *KLF4*). From those nine genes, we selected five candidates for validation by quantitative real-time PCR analysis. Expression of all five transcripts was reduced in mutant SCA7 astrocytes; however, expression of the *RELN* gene was most dramatically affected (Fig. 2*A*). Reelin mRNA levels were reduced by 69%, 73%, and 67% when measured with PCR primer sets spanning the junctions of exons 1/3, 21/22, and 61/62, respectively (Fig. 2*B*). Additionally, Western blot of whole-cell extracts (WCEs) from SCA7 astrocytes demonstrated reduction of RELN protein levels in cells expressing polyQ ATXN7 (Fig. 2*C*).

Polyglutamine Expansion Alters ATXN7 Binding and H2B Monoubiquitination at RELN Promoter. After confirming reduction of RELN gene expression in mutant SCA7 astrocytes, we sought to determine

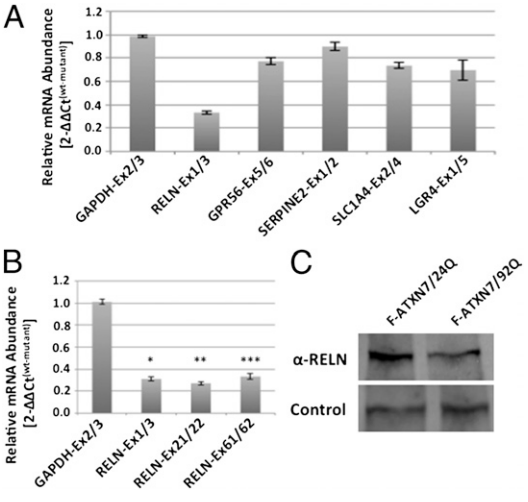

Fig. 2. Expression of polyQ ATXN7 results in the alternative regulation of multiple transcripts. (*A*) Several neural-associated genes are alternatively regulated in mutant SCA7 astrocytes. *P* values for all target genes shown (except GAPDH) were <0.01. (*B*) Down-regulation of the RELN transcript was verified with three real-time PCR primer sets. Error bars represent ± SEM (*$P = 4.34 \times 10^{-43}$, **$P = 3.35 \times 10^{-34}$, ***$P = 1.14 \times 10^{-29}$, two-tailed Student *t* test). (*C*) Immunoblot of WCE demonstrates a reduction in RELN protein levels in mutant SCA7 astrocytes. Equal protein loading was verified relative to a cross-reacting band.

whether regulation of the *RELN* gene occurred through direct association of the ATXN7 protein with the *RELN* promoter. To this end, we used ChIP to quantify the relative association of WT or mutant ATXN7 proteins with the *RELN* promoter in our astrocyte model. Association of WT or mutant ATXN7 with the *RELN* promoter was measured relative to corresponding levels of histone H3, which were normalized to H3 levels at the *β-actin* promoter. Importantly, we did not observe a significant difference in H3 levels at the *RELN* promoter between WT and mutant SCA7 astrocytes (Fig. S1). Polyglutamine expansion reduced occupancy of ATXN7 at −1/+186 bp relative to the *RELN* coding region by 38% (Fig. 3*A*). Interestingly, despite the reduction in polyQ ATXN7 occupancy, the acetylation of histone H3 at lysine 9 and 14 (K9/14) within this region was only marginally reduced in mutant SCA7 astrocytes (Fig. 3*B*). Consistent with our observations at the *RELN* promoter, bulk levels of H3 K9/14 acetylation were also unchanged in mutant SCA7 astrocytes (Fig. 3*D*). The lack of a dramatic change in the acetylation of chromatin within the *RELN* promoter led us to explore the potential influence of polyQ ATXN7 on other SAGA functions.

Given the importance of histone H2B deubiquitination in the regulation of transcriptional initiation/elongation (24) and the H2B deubiquitination activity of the SAGA complex (22, 23, 25), we were interested in determining whether polyglutamine expansion of ATXN7 altered the monoubiquitination of H2B at the *RELN* promoter. We performed ChIP in SCA7 astrocytes with antibodies directed against total or monoubiquitinated (on lysine 120) histone H2B and quantified the relative association with the *RELN* promoter by real-time PCR. Levels of monoubiquitinated H2B at the *RELN* promoter increased in mutant SCA7 astrocytes by 2.20 fold (Fig. 3*C*). Interestingly, bulk H2B monoubiquitination also increased in the mutant SCA7 astrocytes (Fig. 3*D*). These data demonstrate that the *RELN* gene is a target of ATXN7 in astrocytes and that polyglutamine expansion interferes with occupancy of ATXN7 at the *RELN* promoter. Further, diminished binding of polyQ ATXN7 coincides with increased levels of H2B monoubiquitination at the *RELN* promoter without a substantial change in H3K9/14 acetylation. The effects of polyQ ATXN7 expression mirror the changes that occur in global levels of these two histone modifications in mutant SCA7 astrocytes.

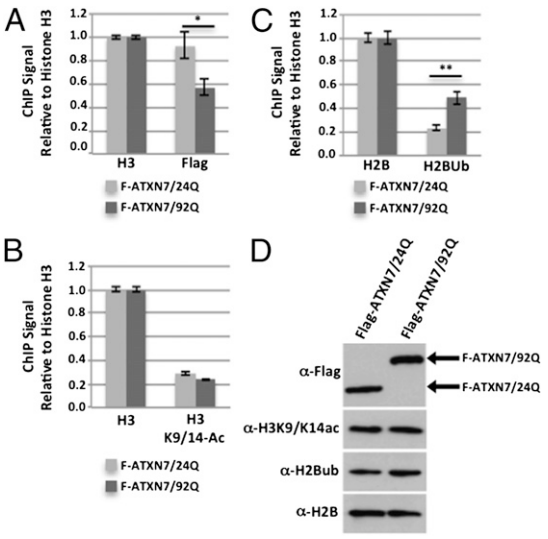

Fig. 3. Polyglutamine expansion of ATXN7 alters chromatin occupancy and histone H2B monoubiquitination at the *RELN* promoter and increases global H2B monoubiquitination. (*A*) Polyglutamine expansion of ATXN7 resulted in a reduction of polyQ ATXN7 occupancy at the RELN promoter. (*B*) Although the change in ATXN7 occupancy on the *RELN* promoter did not substantially alter levels of H3K9/14 acetylation, (*C*) H2B monoubiquitination levels at the RELN promoter increased in mutant SCA7 astrocytes. (*D*) Global H3K9/14 acetylation was unchanged whereas global H2B monoubiquitination was increased in mutant SCA7 astrocytes. ChIP antibodies are shown on the *x*-axes of graphs in *A*–*C*. Histone H3 (*A* and *B*) and H2B (*C*) values shown were normalized to H3 and H2B occupancy within the β-actin promoter, respectively. Error bars represent ± SEM (*$P = 3.62 \times 10^{-34}$, **$P = 2.70 \times 10^{-4}$, two-tailed Student *t* test).

Treatment with Trichostatin a Partially Rescues RELN Gene Transcription and Alters NI Dynamics in Mutant SCA7 Astrocytes. Despite the role of WT ATXN7 as an integral constituent of the SAGA complex (26), polyglutamine expansion of the ATXN7 protein disrupts complex integrity and nucleosomal acetyltransferase function (12, 13). As a result, histone deacetylase inhibitors (HDACis) have been proposed as potential treatments to ameliorate changes in chromatin acetylation resulting from expression of polyglutamine-expanded proteins. We tested three HDACi for their ability to restore RELN mRNA levels in mutant SCA7 astrocytes. Compared with vehicle treatment, trichostatin A (TSA) partially rescued RELN mRNA levels in mutant SCA7 astrocytes (Fig. 4*A*). Surprisingly, the partial rescue occurred when cells received TSA at 200 ng/mL, but not 100 ng/mL or 300 ng/mL, despite similar levels of induced histone H3 acetylation (Fig. S2). In contrast, treatment of mutant SCA7 astrocytes across a range of sodium butyrate or nicotinamide concentrations failed to significantly increase levels of RELN mRNA over their respective vehicle treatments (Fig. 4 *B* and *C*), despite their ability to induce bulk hyperacetylation of histones H3 and H4, respectively (Fig. S2).

Polyglutamine expansion and acetylation have been shown to independently promote the stability and accumulation of the ATXN7 protein (5, 19). Given this information, we sought to determine whether TSA treatment had an effect on either ATXN7 protein levels or NI formation in mutant SCA7 astrocytes. Thus, at 5 d postinfection, we subjected mutant SCA7 astrocytes to 200 ng/mL TSA for 18 h before preparing samples for analysis. To monitor acetylation of polyQ ATXN7, exogenous Flag-ATXN7 proteins were immunoprecipitated with anti-Flag antibodies and immunoblotted with anti-acetylated lysine antibodies. Relative levels of exogenous Flag-ATXN7 protein were determined by immunoblotting input material from the immunoprecipitations. Treatment with TSA under these conditions led to a marginal increase in exogenous polyQ ATXN7 (Fig. 5*A*). Interestingly, the change in polyQ ATXN7 protein levels coincided with an increase in the percentage of Flag-positive mutant SCA7 astrocytes containing at least one NI from 20.6% (vehicle-treated) to 40.6% (Fig. 5*B*). Importantly, TSA treatment did not significantly alter the percentage of Flag-ATXN7–positive cells in the population (Fig. S3). Given our previous findings (Fig. 3*C*), we wanted to determine whether treatment with TSA affected H2B monoubiquitination at the *RELN* promoter. Interestingly, exposure of mutant SCA7 astrocytes to TSA resulted in a 1.58-fold decrease in H2B monoubiquitination within the *RELN* promoter (Fig. 5*C*), which was a substantial restoration of the monoubiquitination levels observed in vehicle-treated WT SCA7 astrocytes. These findings indicate that despite minor effects on Flag-polyQ ATXN7 protein levels, treatment with TSA exerts substantial effects on the dynamics of NI formation and chromatin modification within the *RELN* promoter.

Discussion

Here we report the development of a cell culture system to study the effects of polyQ ATXN7 expression in cultured human astrocytes and provide insight into non–cell-autonomous neurodegeneration in SCA7. An increasing body of evidence has indicated that glial cell dysfunction contributes to pathologic processes associated with polyglutamine expansion disorders (2, 6, 7), including the observation that expression of the polyQ ATXN7 protein under the

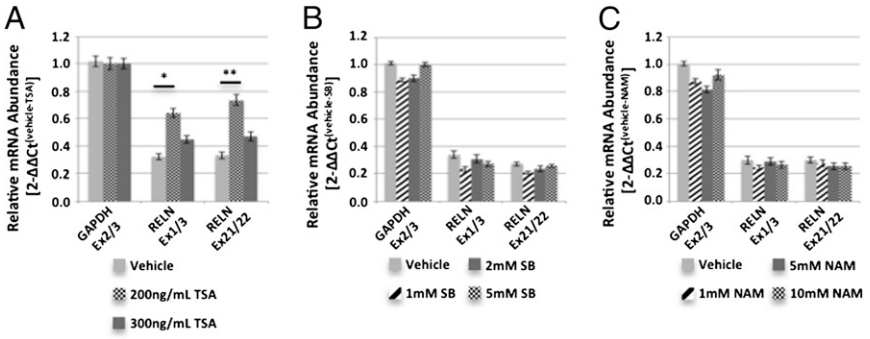

Fig. 4. Treatment with TSA, but not other HDACi, partially restores RELN transcript levels in mutant SCA7 astrocytes. (*A*) Treatment of mutant SCA7 astrocytes to 200 ng/mL TSA led to a significant increase in the amount of RELN transcript compared with vehicle. In contrast, exposure to sodium butyrate (*B*) or nicotinamide (*C*) failed to rescue RELN transcription. Error bars represent ± SEM (*$P = 1.56 \times 10^{-10}$, **$P = 1.04 \times 10^{-10}$, two-tailed Student *t* test).

control of the astrocyte-specific *gfa*2 promoter (8) is sufficient to induce non–cell-autonomous PC degeneration and the development of ataxia in a transgenic mouse model of SCA7 (2). Given the previously documented deleterious effects of polyQ ATXN7 on SAGA integrity and function (12, 13), we sought to identify global transcriptional alterations that occurred in astrocytes following expression of the mutant ATXN7 protein. The relatively small number of transcripts ($n = 21$ coding genes and $n = 8$ noncoding RNAs) that were differentially regulated in mutant SCA7 astrocytes (Tables S1 and S2) was not entirely unexpected given that the median age at SCA7 presentation is 32.5 y, with median disease duration of 20.5 y before death (27). Further, profound global changes in transcription may be expected to cause an earlier disease onset and a more rapid progression. We were, however, intrigued that *RELN* was the most strongly down-regulated gene in mutant SCA7 astrocytes.

Reelin is primarily expressed in the brain and was originally characterized through its role in the direction of neuronal migration and positioning during development (14, 28, 29); however, it has also been shown to play a number of roles in the adult brain, including maintenance of the cerebellar PC layer and synaptic connections in the retina (16, 30), modulation of neuronal glutamate receptor activity (31), direction of neuronal migration (14, 32), and regulation of synaptic plasticity (33). Interestingly, the cerebellar pathology and general phenotype observed in RELN mutant mice are remarkably similar to those of transgenic SCA7 mice (4); yet, further studies would be needed to examine the role of polyQ ATXN7 during development, as well as the role of RELN deficiency in the maintenance of PCs in adults before a more substantial correlation could be made. Further, although the down-regulation of RELN is likely not the sole contributor to the SCA7 phenotype, our findings suggest the potential for decreases in RELN expression, as well as that of other genes, to play a role in SCA7 neurodegeneration.

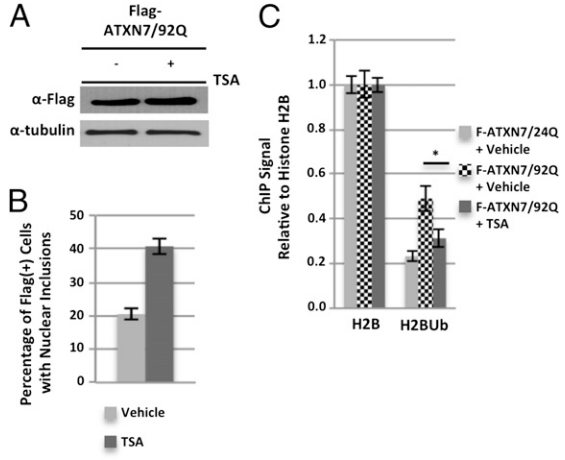

Fig. 5. Treatment with 200 ng/mL TSA alters ATXN7 protein levels, NI dynamics, and H2B monoubiquitination levels at the *RELN* promoter. (*A*) Levels of Flag-polyQ ATXN7 protein were increased in SCA7 astrocytes following 18 h of exposure to 200 ng/mL TSA as shown by immunoblotting WCE with anti-Flag antibodies. (*B*) TSA treatment increased the number of Flag-positive cells with NIs from 20.6% (vehicle) to 40.6% ($P = 6.3 \times 10^{-11}$). (*C*) Histone H2B monoubiquitination in mutant SCA7 astrocytes were reduced to levels similar to those in vehicle-treated WT SCA7 astrocytes following 16 h of exposure to 200 ng/mL TSA (*$P = 1.20 \times 10^{-2}$, two-tailed Student *t* test). Error bars represent ± SEM.

Given the critical role of ATXN7 in the structural integrity of SAGA and its recruitment to target promoters (12, 13, 34), we believe the reduced occupancy of polyQ ATXN7 at the *RELN* promoter (Fig. 3*A*) also reflects diminished SAGA recruitment. Interestingly, given the previously documented loss of nucleosomal acetyltransferase activity in mutant ATXN7-containing SAGA complexes (12, 13), our observations indicate that the acetylation of histone H3 (K9/14) at the *RELN* promoter was only slightly reduced in polyQ SCA7 astrocytes. If the *RELN* promoter were truly not dependent on H3 K9/14 acetylation for its basal regulation (35), a substantial change in acetylation of these residues would not be expected. The increased monoubiquitination of H2B that we observed indicates an alternative mechanism by which polyQ ATXN7 can alter the transcriptional regulation of the *RELN* gene. Surprisingly, although ATXN7 is clearly required for the deubiquitination activity of the SAGA complex and the integrity of the deubiquitination module (25, 36), there has been no evidence published to date that polyglutamine expansion of ATXN7 disrupts this function directly. Instead, we believe the reduction in *RELN* promoter occupancy of polyQ ATXN7-containining SAGA complexes is effectively reducing the presence of the SAGA deubiquitination module at affected promoters. The net effect in polyQ ATXN7-expressing cells is the persistence of H2B monoubiquitination at target promoters, which impedes transcriptional elongation and therefore gene expression. Our findings are consistent with recently published work by Chen et al. (37) in which the authors were able to demonstrate that heterozygous KO of *Gcn5* in *SCA7* knock-in mice accelerated cerebellar degeneration and reduced lifespan. The significance of their report in the context of our findings is that studies provide evidence suggesting that SCA7 pathology does not appear to result solely from alterations to GCN5 HAT activity.

Given the evidence indicating that the loss of acetyltransferase activity is a significant contributor to the pathology of SCA7, as well as other polyglutamine expansion disorders, HDACis have been tested as potential therapeutic agents in laboratory models. Because HDACis other than TSA had been previously shown to induce RELN expression (38), we believed the TSA-specific rescue of RELN expression in our astrocyte system might not simply be the result of increased chromatin acetylation. Findings recently reported by Mookerjee et al. (39) have indicated that acetylation promotes the accumulation of an N-terminal ATXN7 fragment

and insoluble aggregates; however, upon examination of TSA-treated mutant SCA7 astrocytes, we were unable to conclusively demonstrate any difference in the acetylation of the polyQ ATXN7 protein. Instead, we observed an increase in exogenous polyQ ATXN7 protein levels together with a twofold increase in the number of cells containing NIs (Fig. 5). The greater abundance of polyQ ATXN7 may be responsible for the increase in NI-containing cells following TSA treatment; however, further investigation will be required to elucidate the relationship between these two events. Interestingly, experiments in other polyglutamine expansion disorder models have indicated that the formation of NIs is not affected by treatment with SAHA (40), nicotinamide (41), or sodium butyrate (40, 42). The TSA-dependent increase in NI formation and coinciding restoration of H2B monoubiquitination levels may suggest that the mechanism for TSA-dependent rescue of RELN expression involves the sequestration of polyQ ATXN7 into NIs, away from affected promoters in the TSA-treated cells. Depleting mutant ATXN7 from its target promoters in this manner may then allow endogenous WT ATXN7-containing complexes to repopulate promoters and restore expression of affected genes. Despite observations indicating that the presence of NIs precedes or coincides with the onset of disease symptoms in SCA7 mouse models (4, 19), evidence exists suggesting that NIs are not required for disease and may actually be neuroprotective (43, 44). Our results linking TSA treatment to NI formation suggest the interesting possibility that protein acetylation may influence NI formation, however, additional studies are required to characterize the relationship between TSA-dependent alterations in NI dynamics and the expression of genes that are alternatively regulated in SCA7.

Previous studies have reported that RELN expression can be induced by TSA treatment (35); however, similar studies did not report the acetylation of histones H3 (K9/14) and H4 (K5/8/12/16) in the absence of HDACi exposure (38). Although HDACi treatment is sufficient to induce RELN expression artificially, basal regulation of RELN expression does not appear to be SAGA acetylation-dependent. This may suggest histone acetylation independent RELN expression or that other acetyltransferases may compensate for loss of SAGA HAT activity. However, the increase in H2B monoubiquitination we observed at the *RELN* promoter in mutant SCA7 astrocytes may be the primary factor underlying the reduction of RELN expression in these cells. The importance of H2B ubiquitination with regard to RELN expression in this system is further supported by the coincident restoration of H2B monoubiquitination levels and RELN transcription in mutant SCA7 astrocytes following TSA treatment. We have yet to elucidate the mechanism underlying this restoration of H2B monoubiquitination levels; however, it seems reasonable to postulate that hyperacetylation of histones at the *RELN* promoter in response to treatment with TSA would provide additional binding sites for bromodomains within the SAGA complex. Future studies could address the relative binding of WT and polyQ ATXN7-containing SAGA complexes at the *RELN* promoter following TSA treatment to determine if TSA-dependent histone hyperacetylation increased recruitment of SAGA and, ultimately, the restoration of normal levels of monoubiquitinated H2B, at the *RELN* promoter in mutant SCA7 astrocytes.

Materials and Methods

Plasmid Construction. The Flag-tagged ATXN7 expression constructs pSDM253 and pSDM254 were generated in pSDM101 by using a PCR cloning strategy with pTriEx4-Hygro-F-ataxin-7-24Q and pTriEx4-Hygro-F-ataxin-7-92Q (13) as templates, respectively. All plasmid transformations were conducted in *Escherichia coli* strain HB101. Oligonucleotide and primer sequences are given in Table S3.

Cell Culture and Histone Deacetylase Inhibitor Treatment. Artificially immortalized normal human astrocytes (17) were grown in MEM-α (Invitrogen no. 32561–037) supplemented with 10% (vol/vol) FBS (no. 16000-044; Invitrogen). HEK293T/17 cells were acquired from the American Type Culture Collection and grown in DMEM–high glucose (no. 11965-092; Invitrogen) supplemented with 10% FBS, 0.1 mM nonessential amino acids (no. 11140-050; Invitrogen), and 1 mM sodium pyruvate (no. 11360-070; Invitrogen). Cells were passaged according to standard techniques. Effects of HDACi treatment were determined by treating cells with TSA (no. 19-138; Upstate), butyric acid (no. B10,350-0; Aldrich), or nicotinamide (no. N3376; Sigma) in growth medium at indicated concentrations for 18 h before sample collection.

Production and Use of Recombinant Lentiviral Particles. Recombinant lentiviral particles we generated by transient suspension transfection of HEK293T/17 cells with viral transfer and packaging (psPAX2 and pMD2G) vectors. Transfection mixes were prepared with Lipofectamine 2000 (no. 11668-019; Invitrogen) according to the manufacturer. A suspension of HEK293T/17 cells was added to DNA–Lipofectamine 2000 complexes in poly-L-lysine (no. P4832; Sigma)-coated tissue culture dishes. Viral supernatant was collected at 48 and 72 h posttransfection, filtered (0.45-μm pore), and concentrated by ultracentrifugation at 25,000 rpm in an SW-28 rotor (Beckman-Coulter) for 3 h at 4 °C. Viral pellets were resuspended in astrocyte growth medium by rotation overnight at 4 °C before storage at −80 °C. Viral preparations were titered by flow cytometry (FACSCalibur; Becton Dickinson) analysis of EGFP-expressing astrocytes 48 h after infection with serial dilutions of viral stocks. Transduction of experimental samples was performed with 1.0×10^6 astrocytes at a multiplicity of infection of 3 in growth medium supplemented with 2 μg/mL Polybrene (no. 107689; Sigma). To ensure homogeneity of transduced populations during experiments, EGFP-positive cell numbers were measured on the same day cells were harvested for all experiments.

Preparation of Cell Extracts and Western Blotting. WCEs were prepared for Western blotting by boiling cell pellets in Laemmli buffer (45). Proteins were analyzed by electrophoretic separation on SDS/PAGE gels, transfer to nitrocellulose membranes (no. RPN303D; GE Healthcare), and immunoblot with indicated antibodies. Equal amounts of total protein were loaded per lane for each Western blot.

RNA Isolation, Microarray Data Analysis, and Real-Time Quantitative PCR. Small RNA-depleted total RNA (large RNA) was isolated from cultured cells with the miRvana miRNA Isolation Kit (no. AM1560; Ambion) 6 d after infection. Genes that were differentially expressed between astrocytes expressing Flag-ATXN7/24Q (WT SCA7 astrocytes), Flag-ATXN7/92Q (mutant SCA7 astrocytes), and astrocytes transduced with the empty lentiviral vector (vector control) were identified from Affymetrix Gene 1.0 ST microarray data at a 20% false discovery rate (FDR) from pairwise comparisons using Bioconductor software (46). Specifically, we used Robust Multichip Average within the *oligo* package to arrive at normalized, background-subtracted, and probe affinity-corrected relative gene expression levels. The *limma* package was used to determine FDR-corrected *P* values associated with differential expression changes. We then applied a 0.2 FDR cutoff for each pairwise comparison, which included (comparison A) mutant vs. WT (comparison B) mutant vs. vector control and (comparison C) WT vs. vector control. We arrived at a list of alternatively regulated genes by taking the union of genes from comparison A and comparison B and excluding all genes that appeared in comparison C. Large RNA was used as a template for cDNA synthesis by using the VILO RT-PCR kit (no. 11754-050; Invitrogen). Expression of RNA transcripts were evaluated by quantification of cDNA samples with gene-specific primer sets by real-time PCR. Real-time PCR was conducted with a SYBR Green/Taq polymerase reaction mix (no. 170-8884; Bio-Rad) in a MyIQ real-time PCR detection system (Bio-Rad). Data were collected and analyzed with thermal cycler software (BioRad). Data shown represent relative quantitative comparisons of transcript abundance as calculated by the $2^{-\Delta\Delta Ct}$ method using GAPDH as the reference gene (47). Primer sequences are given in Table S3.

ChIP. ChIP was performed according to published protocols with modifications (48). Cells (2.0×10^7 per sample) were fixed for 4 min in 1% formaldehyde. Chromatin was fragmented by digestion with 25 U/mL MNase (no. 70196Y; USB) for 10 min at 37 °C before being solubilized by six rounds of sonication consisting of 20 pulses per round at 20% output with a 60% duty cycle (Sonifier model 250; Branson). DNA was isolated from ChIP samples with a PCR purification kit (no. K3100-02; Invitrogen).

Antibodies. The following antibodies were used as indicated for Western blot, immunostaining, or ChIP. Anti-Flag (no. F3156, Western blot; no. F1804,

immunostaining and ChIP; Sigma), anti-GCN5 (no. 607202; Biolegend), anti-histone H2B (no. 17-10054; Millipore), anti-histone H2B ubiquitinated on lysine 120 (no.17-650; Millipore), anti-histone H3 (no. 39163; Active Motif), anti-histone H3 acetylated on lysine 9/14 (no. 06-599; Millipore), anti-histone H4 acetylated on lysine 16 (no. 39167; Active Motif), or anti-reelin (no. ab78540; Abcam). Anti-mouse Cy3 (no. 715-095-150; Jackson ImmunoResearch) and anti-rabbit DyLight649 (no.111-495-003; Jackson ImmunoResearch) were used as secondary antibodies for immunostaining. Horseradish peroxidase-conjugated anti-mouse IgG (no. NA931V; GE Healthcare) or anti-rabbit IgG (no. NA934V; GE Healthcare) were used to detect primary antibody binding in Western blots following application of ECL (no. 34080; Pierce).

Immunofluorescence Microscopy. Cells were cultured on poly-L-lysine–coated glass coverslips (no. 12-545-100; Fisher) for 24 to 48 h before fixation according to previously published methods (49). Cell margins were shown with Alexa 488-Phalloidin (no. A12379; Invitrogen) and nuclei were stained with Hoechst 33342 dye (no. B2261; Sigma). Coverslips were inverted onto glass microslides in ProLong Gold mounting medium (no. P36934; Invitrogen), which was allowed to set overnight before coverslips were sealed with clear fingernail polish. Slides were observed on a DeltaVision wide-field microscope (Applied Precision) and images were acquired with SoftWoRx software (Applied Precision). Images shown represent condensed *z*-stacks that were taken at a magnification of 600× under oil immersion.

ACKNOWLEDGMENTS. We thank Dr. Didier Trono for providing vectors for the lentiviral gene delivery system; Dr. Isa Hussaini for providing the immortalized human astrocytes; Drs. Marty Mayo, Jeff Smith, Dan Foltz, and Scott Zeitlin for their input into the development of experiments; and Dr. Eva J. Waller for critical reading of the manuscript. This work was supported by National Institutes of Health Grant R01NS049065 (to P.A.G.) and National Institute of General Medical Sciences Grant T32-GM08136 (to S.D.M.).

1. David G, et al. (1997) Cloning of the SCA7 gene reveals a highly unstable CAG repeat expansion. *Nat Genet* 17(1):65–70.
2. Custer SK, et al. (2006) Bergmann glia expression of polyglutamine-expanded ataxin-7 produces neurodegeneration by impairing glutamate transport. *Nat Neurosci* 9(10): 1302–1311.
3. Yvert G, et al. (2000) Expanded polyglutamines induce neurodegeneration and trans-neuronal alterations in cerebellum and retina of SCA7 transgenic mice. *Hum Mol Genet* 9(17):2491–2506.
4. Garden GA, et al. (2002) Polyglutamine-expanded ataxin-7 promotes non-cell-autonomous Purkinje cell degeneration and displays proteolytic cleavage in ataxic transgenic mice. *J Neurosci* 22(12):4897–4905.
5. Yoo SY, et al. (2003) SCA7 knockin mice model human SCA7 and reveal gradual accumulation of mutant ataxin-7 in neurons and abnormalities in short-term plasticity. *Neuron* 37(3):383–401.
6. Lobsiger CS, Cleveland DW (2007) Glial cells as intrinsic components of non-cell-autonomous neurodegenerative disease. *Nat Neurosci* 10(11):1355–1360.
7. Bradford J, et al. (2009) Expression of mutant huntingtin in mouse brain astrocytes causes age-dependent neurological symptoms. *Proc Natl Acad Sci USA* 106(52): 22480–22485.
8. Brenner M, Kisseberth WC, Su Y, Besnard F, Messing A (1994) GFAP promoter directs astrocyte-specific expression in transgenic mice. *J Neurosci* 14(3 pt 1):1030–1037.
9. Eroglu C, Barres BA (2010) Regulation of synaptic connectivity by glia. *Nature* 468 (7321):223–231.
10. Barres BA (2008) The mystery and magic of glia: A perspective on their roles in health and disease. *Neuron* 60(3):430–440.
11. Haydon PG (2001) GLIA: listening and talking to the synapse. *Nat Rev Neurosci* 2(3): 185–193.
12. McMahon SJ, Pray-Grant MG, Schieltz D, Yates JR, 3rd, Grant PA (2005) Polyglutamine-expanded spinocerebellar ataxia-7 protein disrupts normal SAGA and SLIK histone acetyltransferase activity. *Proc Natl Acad Sci USA* 102(24):8478–8482.
13. Palhan VB, et al. (2005) Polyglutamine-expanded ataxin-7 inhibits STAGA histone acetyltransferase activity to produce retinal degeneration. *Proc Natl Acad Sci USA* 102 (24):8472–8477.
14. D'Arcangelo G, et al. (1995) A protein related to extracellular matrix proteins deleted in the mouse mutant reeler. *Nature* 374:719–723.
15. Hong SE, et al. (2000) Autosomal recessive lissencephaly with cerebellar hypoplasia is associated with human RELN mutations. *Nat Genet* 26(1):93–96.
16. Miyata T, et al. (2010) Migration, early axonogenesis, and Reelin-dependent layer-forming behavior of early/posterior-born Purkinje cells in the developing mouse lateral cerebellum. *Neural Dev* 5:23.
17. Sonoda Y, et al. (2001) Formation of intracranial tumors by genetically modified human astrocytes defines four pathways critical in the development of human anaplastic astrocytoma. *Cancer Res* 61(13):4956–4960.
18. Orr HT, Zoghbi HY (2007) Trinucleotide repeat disorders. *Annu Rev Neurosci* 30: 575–621.
19. Yvert G, et al. (2001) SCA7 mouse models show selective stabilization of mutant ataxin-7 and similar cellular responses in different neuronal cell types. *Hum Mol Genet* 10(16):1679–1692.
20. Grant PA, et al. (1997) Yeast Gcn5 functions in two multisubunit complexes to acetylate nucleosomal histones: Characterization of an Ada complex and the SAGA (Spt/Ada) complex. *Genes Dev* 11(13):1640–1650.
21. Martinez E, Kundu TK, Fu J, Roeder RG (1998) A human SPT3-TAFII31-GCN5-L acetylase complex distinct from transcription factor IID. *J Biol Chem* 273(37):23781–23785.
22. Daniel JA, et al. (2004) Deubiquitination of histone H2B by a yeast acetyltransferase complex regulates transcription. *J Biol Chem* 279(3):1867–1871.
23. Zhao Y, et al. (2008) A TFTC/STAGA module mediates histone H2A and H2B deubiquitination, coactivates nuclear receptors, and counteracts heterochromatin silencing. *Mol Cell* 29(1):92–101.
24. Wyce A, et al. (2007) H2B ubiquitylation acts as a barrier to Ctk1 nucleosomal recruitment prior to removal by Ubp8 within a SAGA-related complex. *Mol Cell* 27(2): 275–288.
25. Lee KK, Swanson SK, Florens L, Washburn MP, Workman JL (2009) Yeast Sgf73/Ataxin-7 serves to anchor the deubiquitination module into both SAGA and Slik(SALSA) HAT complexes. *Epigenetics Chromatin* 2(1):2.
26. Helmlinger D, et al. (2004) Ataxin-7 is a subunit of GCN5 histone acetyltransferase-containing complexes. *Hum Mol Genet* 13(12):1257–1265.
27. Giunti P, et al. (1999) Molecular and clinical study of 18 families with ADCA type II: Evidence for genetic heterogeneity and de novo mutation. *Am J Hum Genet* 64(6): 1594–1603.
28. Curran T, D'Arcangelo G (1998) Role of reelin in the control of brain development. *Brain Res Brain Res Rev* 26(2-3):285–294.
29. Förster E, et al. (2006) Recent progress in understanding the role of Reelin in radial neuronal migration, with specific emphasis on the dentate gyrus. *Eur J Neurosci* 23(4): 901–909.
30. Rice DS, et al. (2001) The reelin pathway modulates the structure and function of retinal synaptic circuitry. *Neuron* 31(6):929–941.
31. Qiu S, Zhao LF, Korwek KM, Weeber EJ (2006) Differential reelin-induced enhancement of NMDA and AMPA receptor activity in the adult hippocampus. *J Neurosci* 26(50):12943–12955.
32. Rice DS, Curran T (2001) Role of the reelin signaling pathway in central nervous system development. *Annu Rev Neurosci* 24:1005–1039.
33. Herz J, Chen Y (2006) Reelin lipoprotein receptors and synaptic plasticity. *Nat Rev Neurosci* 7:850–859.
34. Shukla A, Bajwa P, Bhaumik SR (2006) SAGA-associated Sgf73p facilitates formation of the preinitiation complex assembly at the promoters either in a HAT-dependent or independent manner in vivo. *Nucleic Acids Res* 34(21):6225–6232.
35. Chen Y, Sharma RP, Costa RH, Costa E, Grayson DR (2002) On the epigenetic regulation of the human reelin promoter. *Nucleic Acids Res* 30(13):2930–2939.
36. Köhler A, Schneider M, Cabal GG, Nehrbass U, Hurt E (2008) Yeast Ataxin-7 links histone deubiquitination with gene gating and mRNA export. *Nat Cell Biol* 10(6): 707–715.
37. Chen YC, et al. (2012) Gcn5 loss-of-function accelerates cerebellar and retinal degeneration in a SCA7 mouse model. *Hum Mol Genet* 21(2):394–405.
38. Mitchell CP, Chen Y, Kundakovic M, Costa E, Grayson DR (2005) Histone deacetylase inhibitors decrease reelin promoter methylation in vitro. *J Neurochem* 93(2):483–492.
39. Mookerjee S, et al. (2009) Posttranslational modification of ataxin-7 at lysine 257 prevents autophagy-mediated turnover of an N-terminal caspase-7 cleavage fragment. *J Neurosci* 29(48):15134–15144.
40. Steffan JS, et al. (2001) Histone deacetylase inhibitors arrest polyglutamine-dependent neurodegeneration in Drosophila. *Nature* 413(6857):739–743.
41. Hathorn T, Snyder-Keller A, Messer A (2011) Nicotinamide improves motor deficits and upregulates PGC-1α and BDNF gene expression in a mouse model of Huntington's disease. *Neurobiol Dis* 41(1):43–50.
42. Chou AH, Chen SY, Yeh TH, Weng YH, Wang HL (2011) HDAC inhibitor sodium butyrate reverses transcriptional downregulation and ameliorates ataxic symptoms in a transgenic mouse model of SCA3. *Neurobiol Dis* 41(2):481–488.
43. Arrasate M, Mitra S, Schweitzer ES, Segal MR, Finkbeiner S (2004) Inclusion body formation reduces levels of mutant huntingtin and the risk of neuronal death. *Nature* 431(7010):805–810.
44. Bowman AB, Yoo SY, Dantuma NP, Zoghbi HY (2005) Neuronal dysfunction in a polyglutamine disease model occurs in the absence of ubiquitin-proteasome system impairment and inversely correlates with the degree of nuclear inclusion formation. *Hum Mol Genet* 14(5):679–691.
45. Laemmli UK (1970) Cleavage of structural proteins during the assembly of the head of bacteriophage T4. *Nature* 227(5259):680–685.
46. Gentleman RC, et al. (2004) Bioconductor: Open software development for computational biology and bioinformatics. *Genome Biol* 5(10):R80.
47. Livak KJ, Schmittgen TD (2001) Analysis of relative gene expression data using real-time quantitative PCR and the 2(-Δ Δ C(T)) Method. *Methods* 25(4):402–408.
48. Aparicio O, et al. (2001) *Chromatin Immunoprecipitation for Determining the Association of Proteins with Specific Genomic Sequences in Vivo* (Wiley, New York).
49. Miller SA, Johnson ML, Stukenberg PT (2008) Kinetochore attachments require an interaction between unstructured tails on microtubules and Ndc80(Hec1). *Curr Biol* 18(22):1785–1791.